

First principles study of B₇N₅ as high capacity electrode material for K-ion batteries

Yu Xiong,^a Yuhang Wang,^a Ninggui Ma,^a Yaqin Zhang,^a Shuang Luo^a and Jun Fan^{a,b,*}

^a *Department of Materials Science and Engineering, City University of Hong Kong, Hong Kong, China.*

^b *Center for Advance Nuclear Safety and Sustainable Department, City University of Hong Kong, Hong Kong, China*

*Corresponding author

Email address: junfan@cityu.edu.hk (Jun Fan)

Fig. S1

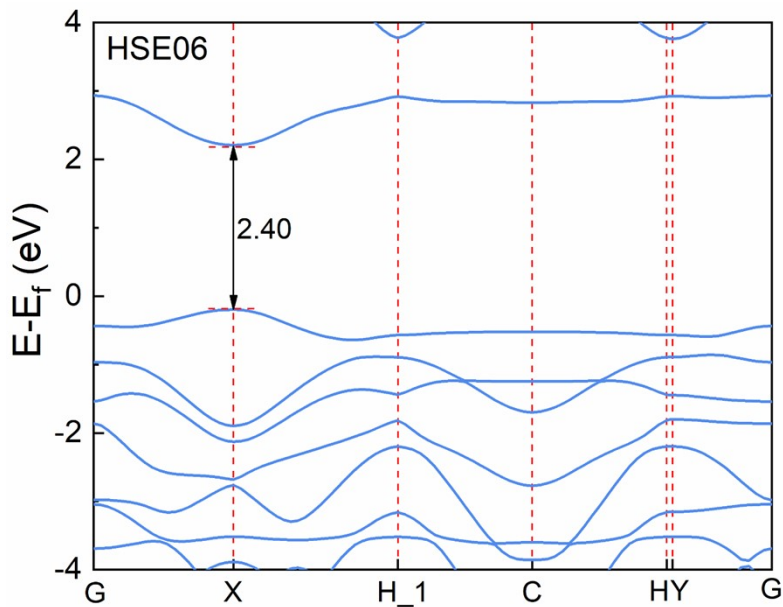


Fig. S1 The band structure of B₇N₅ via HSE06 method.

Fig. S2

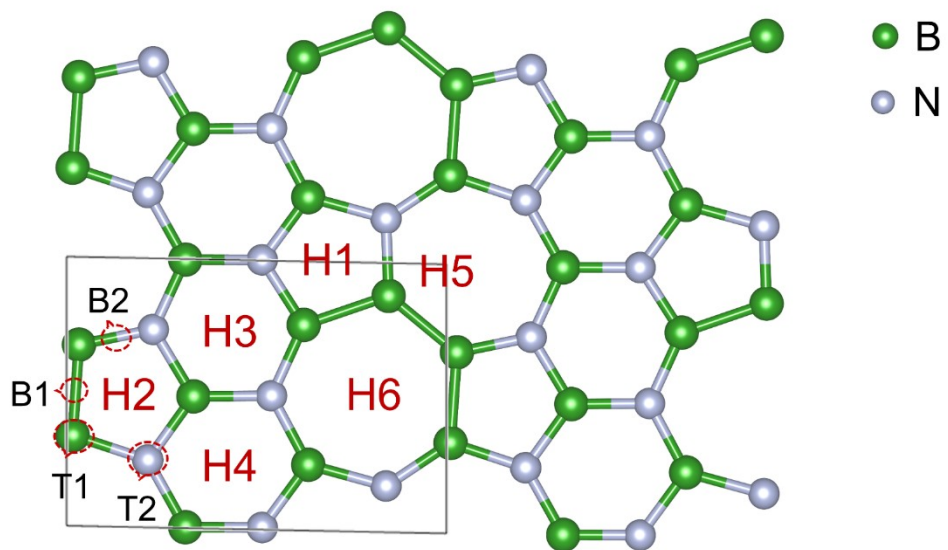


Fig. S2 The possible adsorption hollow, top and bridge sites for metal atom on B₇N₅.

Fig. S3

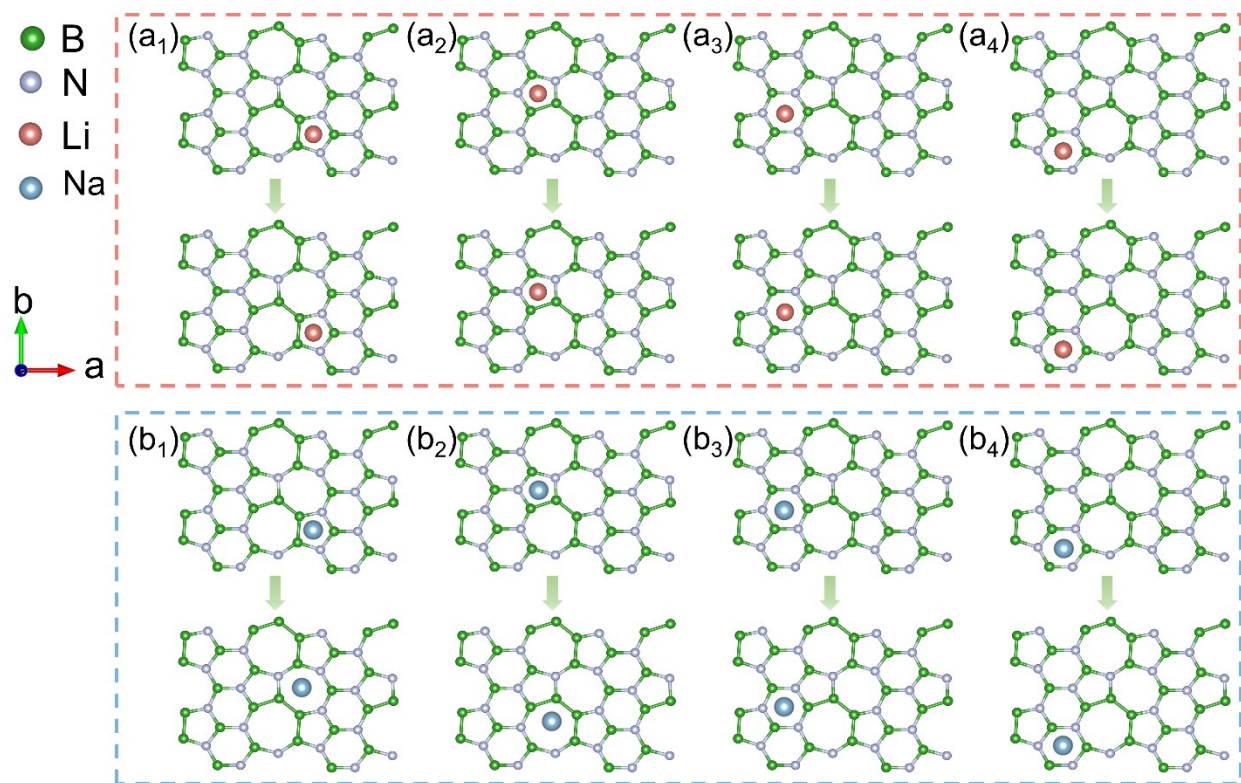


Fig. S3 The initial structures (first row) and optimized structures (second row) of a single (a) Li, (b) Na atom adsorbed of different hollow sites (H1, H2, H3 and H4) on B_7N_5 .

Fig. S4

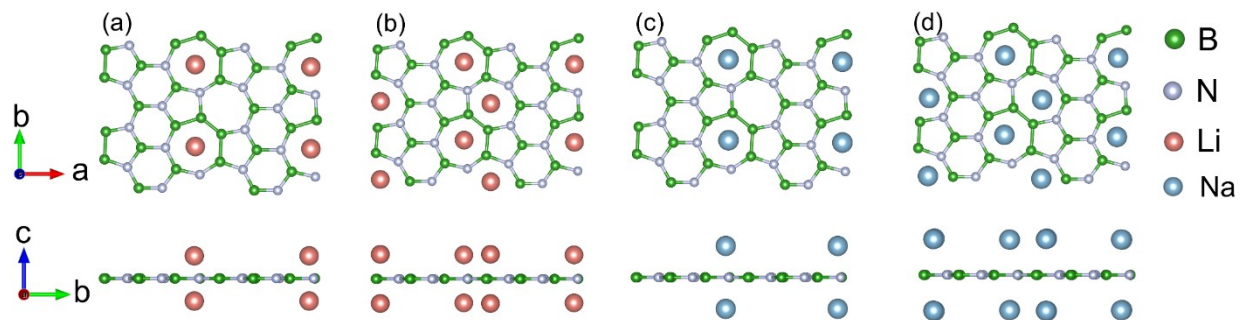


Fig. S4 The optimized structure of top view and side view of (a) $B_7N_5Li_2$, (b) $B_7N_5Li_4$, (c) $B_7N_5Na_2$, (d) $B_7N_5Na_4$.

Fig. S5

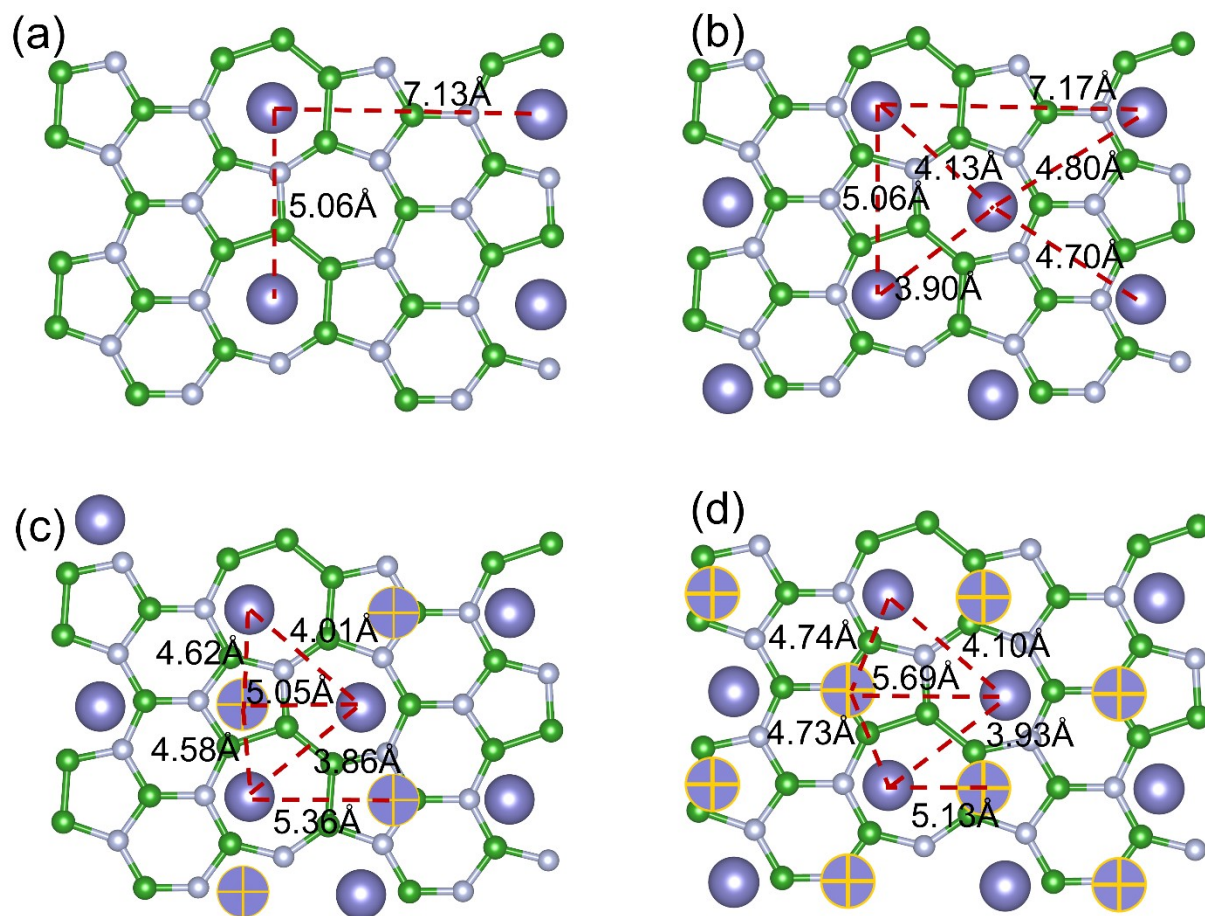


Fig. S5 The distances between K atoms for (a) $B_7N_5K_2$, (b) $B_7N_5K_4$, (c) $B_7N_5K_6$ and (d) $B_7N_5K_8$.

Fig. S6

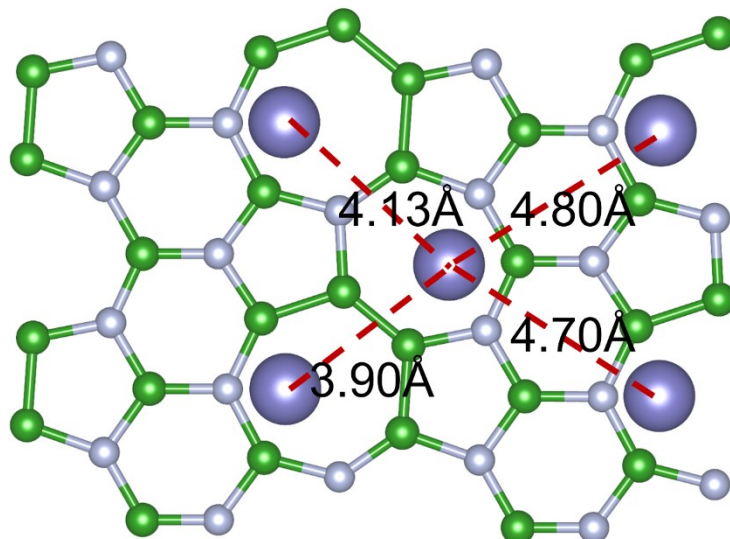


Fig. S6 The distances of the optimized first layer of K adsorption on B₇N₅.

The distance mismatch parameter was defined to investigate the adsorption performance of the B₇N₅ substrate. As shown in Fig. S6, the average distance (d_1) for first layer of K atoms adsorbed on B₇N₅ is 4.38 Å, as well as Li (4.58 Å) and Na (4.42 Å). The equilibrium distance (d_2) is 4.36 Å for K. Therefore, the distance mismatch (Δd) can be calculated by the following equation:

$$\Delta d = |d_1 - d_2|/d_1 \quad (1)$$

The distance mismatches for different metal systems are 17.5% (Li), 10.0% (Na) and 0.5% (K).

Fig. S7

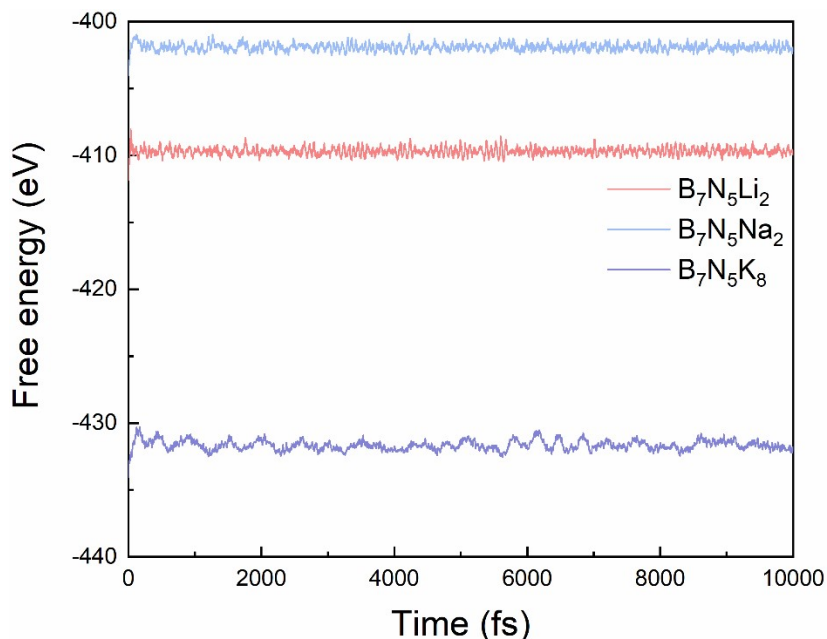


Fig. S7 The variation of the free energy in the AIMD simulations for $B_7N_5Li_2$, $B_7N_5Na_2$ and $B_7N_5K_8$.

The thermal stability of the B_7N_5 monolayer after metal layer adsorption is essential for the safety of battery operation. Therefore, the AIMD simulations of the fully charged (Li, Na, K) systems are conducted to check the thermal dynamical stability of the end geometries ($B_7N_5Li_2$, $B_7N_5Na_2$, $B_7N_5K_8$) at 300 K. As shown in Fig. S7, there is no sharp drop or rise for the free energy of three systems during the simulation, demonstrating the stability of all the end geometries. The thermal stability is also conveyed that the B_7N_5 monolayer is an outstanding candidate electrode material for metal-ion batteries.

Table S1

Table S1. The calculated elastic constant (C_{ij}) values of B_7N_5 .

Method	C_{11}	C_{12}	C_{16}	C_{22}	C_{26}	C_{66}
Stress-strain	231.64	60.48	0.58	221.76	-0.88	90.16
Energy-strain	234.45	61.80	0.44	224.50	-0.82	91.13

Table S2

Table S2. The Young's modulus (Y) and Poisson's ratio (ν) of B_7N_5 .

Method	Y_{min} (N/m)	Y_{max} (N/m)	ν_{min}	ν_{max}
Stress-strain	205.85	222.34	0.23	0.27
Energy-strain	208.11	224.84	0.23	0.28

Table S3

Table S3. Theoretically calculated adsorption energy, distance between Li/Na/K and B₇N₅, charge transfer from Li/Na/K to B₇N₅ at different adsorption hollow site.

Metal	Adsorption site	E_{ad} (eV)	Distance (Å)	Q (e)
Li	H1	-0.07	1.85	0.781
	H2	-0.10	1.84	0.761
	H3	0.15	1.73	0.772
	H4	0.22	1.74	0.807
	H5	-0.46	1.51	0.786
	H6	-0.47	1.50	0.759
Na	H1	-0.14	\	\
	H2	-0.18	\	\
	H3	0.31	2.21	0.796
	H4	0.35	2.22	0.811
	H5	-0.14	2.08	0.737
	H6	-0.17	2.10	0.692
K	H1	-0.69	\	\
	H2	-0.65	\	\
	H3	-0.40	2.57	0.854
	H4	-0.37	2.59	0.857
	H5	-0.69	2.48	0.784
	H6	-0.65	2.49	0.779

Table S4

Table S4. Theoretically calculated diffusion coefficient on the surface of B₇N₅ at 300 K.

Metal	<i>l</i> (Å)	E_a (eV)	Diffusion coefficient (cm²s⁻¹)
Li	3.06	0.49	5.96×10 ⁻¹¹
Na	2.88	0.13	5.23×10 ⁻⁰⁵
K	2.83	0.10	1.68×10 ⁻⁰⁴

Table S5

Table S5. The calculated adsorption energy, charge transfer and distance between metal atoms and B₇N₅ for adsorption different Li, Na and K layers.

Metal	Layer	Adsorption sites	Total numbers	E _{ads} (eV)	Q _{ave} (e)	Distance (Å)
Li	One layer	H6	8	-0.66	0.72	1.40
		H5+H6	16	0.23	\	1.54
Na	One layer	H6	8	-0.22	0.56	1.97
		H5+H6	16	0.07	\	2.22
K	One layer	H6	8	-0.48	0.52	2.45
		H5+H6	16	-0.24	0.29	2.70
	Two layers	H3+H5+H6	24	-0.05	0.21	2.71/6.37
		H3+H4+H5+H6	32	-0.14	0.17	2.68/6.53/7.15
	Three layers	H2+H3+ H4+H5+H6	40	0.37	\	2.48/5.82/7.89

Table S6Table S6. The free energies of different B₇N₅ structures after adsorbing Li/Na/K metal atoms.

Material	Formation energy (eV)	Material	Formation energy (eV)
B ₇ N ₅ Li _{0.5}	-0.50	B ₇ N ₅ Li ₁	-0.50
B ₇ N ₅ Li _{1.5}	-0.61	B ₇ N ₅ Li ₂	-0.65
B ₇ N ₅ Na _{0.5}	-0.33	B ₇ N ₅ Na ₁	-0.26
B ₇ N ₅ Na _{1.5}	-0.23	B ₇ N ₅ Na ₂	-0.21
B ₇ N ₅ K _{0.5}	-0.70	B ₇ N ₅ K ₁	-0.57
B ₇ N ₅ K _{1.5}	-0.50	B ₇ N ₅ K ₂	-0.48
B ₇ N ₅ K _{2.5}	-0.42	B ₇ N ₅ K ₃	-0.41
B ₇ N ₅ K _{3.5}	-0.36	B ₇ N ₅ K ₄	-0.36
B ₇ N ₅ K _{4.5}	-0.31	B ₇ N ₅ K ₅	-0.27
B ₇ N ₅ K _{5.5}	-0.26	B ₇ N ₅ K ₆	-0.25
B ₇ N ₅ K _{6.5}	-0.24	B ₇ N ₅ K ₇	-0.22
B ₇ N ₅ K _{7.5}	-0.24	B ₇ N ₅ K ₈	-0.22

Table S7

Table S7. The lattice constant and change in lattice constant (%) after adsorption different metal on B₇N₅.

System	<i>a</i> (Å)	<i>b</i> (Å)	Change in <i>a</i> (%)	Change in <i>b</i> (%)
B ₇ N ₅ Li ₂	10.10	14.27	0.40	0.35
B ₇ N ₅ Na ₂	10.11	14.29	0.49	0.49
B ₇ N ₅ K ₂	10.10	14.26	0.40	0.28
B ₇ N ₅ K ₄	10.09	14.30	0.30	0.56
B ₇ N ₅ K ₆	10.10	14.30	0.40	0.63
B ₇ N ₅ K ₈	10.14	14.41	0.79	1.32

Table S8

Table S8. Comparison of diffusion energy barriers, capacity and open circuit voltage (OCV) for various K-ion batteries.

Materials	Diffusion barriers (eV)	Capacity (mAh/g)	OCV (V)
B ₇ N ₅ (this work)	0.10	1471.5	0.14
BP ¹	0.16	570	0.28
1H-BeP ₂ ²	0.13	377.5	0.34
Graphit ³	0.26	273	-
Si ₃ C ⁴	0.18	836	0.5
VS ₂ ⁵	0.06	466	-
Ti ₃ C ₂ ⁶	0.10	191.8	0.12
TiS ₂ ⁷	0.09	957	1.0
TiF ₂ ⁸	0.25	208	0.64
Ti ₂ BN ₂ ⁹	0.37	398	0.16
Ti ₂ PS ₂ ¹⁰	0.07	281	0.28
Nb ₂ N ¹¹	0.02	201	0.5
SnSe ₂ ¹²	0.11	387	0.48
SnC ¹³	0.17	410	0.41
MoS ₂ ¹⁴	0.06	334	0.24
β-Sb ¹⁵	0.09	440.2	0.09
BeNC ₁₆ ¹⁶	0.5	747.3	0.48

Table S9Table S9 The structural information of the B₇N₅ monolayer

Compound	Atomic position			
B ₇ N ₅ a = 5.03 Å b = 7.11 Å c = 20.00 Å α = 90.0° β = 90.0° γ = 88.83°	B	0.5130	0.6481	0.5
	B	0.9037	0.1317	0.5
	B	0.2663	0.3444	0.5
	B	0.0235	0.6697	0.5
	B	0.3587	0.9678	0.5
	B	0.6977	0.9511	0.5
	B	0.7886	0.3564	0.5
	N	0.7602	0.7546	0.5
	N	0.5213	0.4417	0.5
	N	0.0286	0.4664	0.5
	N	0.2717	0.7691	0.5
N	0.1928	0.1387	0.5	

Table S10

Table S10 The value of the high symmetry points used to plot the band structures of the B₇N₅ monolayer

High symmetry point	Value		
G	0.00	0.00	0.00
X	0.50	0.00	0.00
H_1	0.98	0.49	0.00
C	0.50	0.50	0.00
H	0.02	0.51	0.00
Y	0.00	0.50	0.00

REFERENCES

1. H. R. Jiang, W. Shyy, M. Liu, L. Wei, M. C. Wu and T. S. Zhao, *J. Mater. Chem. A*, 2017, **5**, 672-679.
2. Q.-H. Qiu, S.-Y. Wu, G.-J. Zhang, L. Yan and Z.-T. Wei, *Comput. Mater. Sci.*, 2023, **216**, 111868.
3. Z. Xu, X. Lv, J. Chen, L. Jiang, Y. Lai and J. Li, *Carbon*, 2016, **107**, 885-894.
4. Y. Wang and Y. Li, *J. Mater. Chem. A*, 2020, **8**, 4274-4282.
5. D. Wang, Y. Liu, X. Meng, Y. Wei, Y. Zhao, Q. Pang and G. Chen, *J. Mater. Chem. A*, 2017, **5**, 21370-21377.
6. D. Er, J. Li, M. Naguib, Y. Gogotsi and V. B. Shenoy, *ACS Appl Mater Interfaces*, 2014, **6**, 11173-11179.
7. A. Samad, A. Shafique and Y. H. Shin, *Nanotechnology*, 2017, **28**, 175401.
8. M. Zhou, Y. Shen, J. Liu, L. Lv, Y. Zhang, X. Meng, X. Yang, Y. Zheng and Z. Zhou, *Vacuum*, 2023, **210**, 111822.
9. B. Liang, N. Ma, Y. Wang, T. Wang and J. Fan, *Appl. Surf. Sci.*, 2022, **599**, 153927.
10. B. Ge, B. Chen and L. Li, *Appl. Surf. Sci.*, 2021, **550**, 149177.
11. Y. Wang, W. Tian, H. Zhang and Y. Wang, *Phys. Chem. Chem. Phys.*, 2021, **23**, 12288-12295.
12. J. Rehman, X. F. Fan, M. K. Butt, A. Laref, V. A. Dinh and W. T. Zheng, *Appl. Surf. Sci.*, 2021, **566**, 150522.
13. J. Rehman, X. Fan, A. Laref and W. T. Zheng, *ChemElectroChem*, 2020, **7**, 3832-3838.
14. J. Rehman, X. Fan, A. Laref, V. A. Dinh and W. T. Zheng, *J. Alloys Compd.*, 2021, **865**, 158782.
15. G. A. Shaikh, D. Cornil, S. K. Gupta, R. Ahuja and P. N. Gajjar, *Energy & Fuels*, 2022, **36**, 7087-7095.
16. S. Ullah, P. A. Denis and F. Sato, *Int J Quantum Chem*, 2019, **119**, e25900.